

## Full Length Article

# Simulations of methanol fueled locomotive engine using high pressure co-axial direct injection system



Dhananjay Kumar <sup>a</sup>, Hardikk Valera <sup>a</sup>, Anirudh Gautam <sup>b</sup>, Avinash Kumar Agarwal <sup>a,\*</sup>

<sup>a</sup> *Engine Research Laboratory, Department of Mechanical Engineering, Indian Institute of Technology Kanpur, Kanpur 208016, India*

<sup>b</sup> *Research Design and Standards Organization, Lucknow, India*

## ARTICLE INFO

**Keywords:**

Methanol  
Locomotive engine  
Simulations  
High pressure direct injection  
Co-axial injector  
Engine performance  
Emissions  
Combustion characteristics

## ABSTRACT

Methanol has emerged as a strong alternate fuel candidate, which can meet future fuel requirements for locomotive traction. Simulation approach is an excellent tool for preliminary technical feasibility assessment of alternative fuels compared to time consuming experiments. The objective of this study was therefore to assess the feasibility of 90% diesel displacement by methanol (on energy basis) in the ALCO-251 locomotive engines, the workhorse of Indian Railways (IR). In the first phase of this study, base model of ALCO-251 locomotive engine was prepared in 1-D simulation software (GT-Power), which was validated using the experimental data of mineral diesel provided by Research Designs and Standards Organization (RDSO), which is the R&D wing of IR. Locomotive engine works on eight different engine speeds at different notches: 350 rpm (1st Notch), 450 rpm (2nd Notch), 550 rpm (3rd Notch), 650 rpm (4th Notch), 750 rpm (5th Notch), 850 rpm (6th Notch), 950 rpm (7th Notch), 1050 rpm (8th Notch). In the second phase of the study using this validated model, a co-axial injector was used where methanol was used as the primary fuel, and diesel was used as the secondary fuel for pilot injection using Co-axial High Pressure Direct Injection (HPDI) method. For simulations, methanol and diesel injectors were housed in a single injector body of the co-axial injector, but they had individual controls. Co-axial injector was actuated such that first it injected diesel in hot air-environment to initiate the combustion, followed by injection of methanol as the main motive fuel. Base model simulated the engine performance, emissions, and combustion characteristics quite well, which were in good agreement with the experimental data. Pareto optimized dimensions of the co-axial injector were 0.486 mm nozzle hole diameter, and 3 holes for pilot diesel injection, and 0.544 mm nozzle hole diameter, and 5 holes for methanol injection. HPDI of Methanol with Pilot Diesel Injection Model with optimized injector dimensions exhibited in-cylinder pressure curve shapes similar to the base model with similar/ superior torque characteristics, higher brake thermal efficiency, and lower NOx emissions. Inevitably, 1-D simulation for the locomotive engine represented a potential method to achieve similar/ better engine performance, combustion and emission characteristics via this new fuel injection concept, using high pressure co-axial direct injection system.

## 1. Introduction

India has world's third-largest railway network. Total length of the Indian Railway (IR) network is  $\sim$ 70000 route km. IR's revenue increased at a CAGR of  $\sim$ 6.2% during 2008 to 2019 and was US\$ 27.13 billion in 2019 [1]. IR operated 6023 diesel locomotives and 5399 electric locomotives in 2017 [2]. One can observe that diesel locomotives are the main workhorse of IR and would continue to play a major role for at least next couple of decades. Diesel engines are preferred for road transport, rail-roads and marine sectors due to their high-power

density, wide load-speed operating window, and higher fuel conversion efficiencies [3]. These diesel engines, especially locomotives, emit vast amounts of emissions. Central Pollution Control Board (CPCB), Government of India, has prepared a report entitled "Exhaust Emission Benchmarks for Diesel Locomotives on Indian Railways" [4]. As per this report, IR contributed 24.7 million tonnes of carbon dioxide (CO<sub>2</sub>) in 2013, which was  $\sim$ 9.7% of total CO<sub>2</sub> emissions in India. Currently, emission standards are applied to all light- and heavy-duty vehicles in India, however, there are no emission norms applicable to diesel locomotives as on date. In near future, CPCB is likely to adopt Indian

\* Corresponding author.

E-mail address: [akag@iitk.ac.in](mailto:akag@iitk.ac.in) (A.K. Agarwal).

locomotive emission standards (ILES) norms, and IR would be required to comply with these emission norms for their diesel locomotives.

India currently imports >80% of its petroleum requirements. Petroleum imports are the biggest burden on the exchequer of the nation. A significant fraction of total diesel produced/ imported by India is used in the Rail-road transport sector, which currently stands as ~2.6 million tons per year for locomotive traction alone [5]. Government of India is making concerted efforts to resolve two issues for the Rail-road transport sector: (i) control the emissions from diesel locomotives; and (ii) reduce the diesel import bill by import substitution of fuel required to power these locomotives.

Also, it has been projected in India and elsewhere that Internal Combustion (IC) engines, specially CI engines have outlived their purpose and should be replaced by overhead catenary based power-trains, battery and fuel cell-based drives or hybrid of these. Some of these views have been created by considering well-to-wheel analysis of existing IC engines technologies coupled with petroleum derivatives. However if circular economy, having fuels such as renewable methanol (from biomass, solid waste, carbon sequestration etc.) is considered and the Life Cycle Analysis (LCA) of energy consumption, emissions and Total Cost of Ownership (TCO) are taken into account, the balance tilts in favor of IC engines fuelled by these renewable fuels instead of electrified power-trains. In this context, it is also relevant to point-out that the cost per kW of IC engines is ~USD 50, whereas for pure EVs, it is ~USD 700, and for fuel-cell vehicles (FCVs), it is ~USD 1000. End of life disposal of batteries is a huge concern with battery electric vehicles (BEVs). Advanced engine technologies using alternative renewable fuels are required to address these issues. Methanol is a promising replacement fuel for conventional diesel because it can be prepared from renewable and waste resources, and its usage in the IC engines can lead to significantly lower emissions. India is an agrarian country, and produces considerable amount of agricultural waste, which is disposed-off by burning in a highly inefficient and environmentally polluting manner in-situ, causing widespread environmental and visibility snarls during winters every year. India also has vast reserves of high ash coal and low-value surplus biomass, which are either not utilized or under-utilized, and their inefficient utilisation causes huge environmental concerns. All these readily available, and cheap feedstocks can be used to produce methanol, which can be used as a fuel for diesel locomotives. In addition, methanol can be prepared from the atmospheric CO<sub>2</sub>, CO<sub>2</sub> emitted by the thermal power plants, and from the natural gas, however this route of Methanol production is relatively more expensive. Production of methanol by capturing atmospheric CO<sub>2</sub> could potentially reduce India's contribution to GHG emissions in future, if a cost-effective technology is developed.

Methanol is an oxygenated fuel with higher latent heat of vaporization compared to gasoline/ diesel, which reduces the peak in-cylinder temperature reached in the engine upon combustion. Soot/ particulate matter (PM), oxides of nitrogen (NO<sub>x</sub>), and hydrocarbon (HC) emissions from methanol fuelled engines are also relatively lower than fossil fuel powered engines. Methanol is a zero sulfur fuel hence its utilization in locomotive engines would not emit sulfur oxides (SO<sub>2</sub> and SO<sub>3</sub>), which contribute to the 'Acid Rain' [6,7]. Methanol has higher octane number (~106) compared to commercially available gasoline, however it has relatively lower cetane number than commercially available mineral diesel. It has very high auto-ignition temperature (Methanol: 470 °C, compared to Diesel: 250–450 °C) [8]. Obtaining auto-ignition temperature of methanol in CI engines at the end of compression stroke is difficult; therefore, it is extremely challenging to auto-ignite methanol in CI engines without external assistance or using extremely high compression ratio. Methanol is therefore a preferable fuel for spark ignition (SI) engines [9] and it is difficult to be used in CI engines as a stand-alone fuel. Several researchers explored the potential of methanol fueled SI engines using experiments and computational tools [10–20]. However, methanol research for widespread use in large-bore CI engines is gaining momentum now, especially for rail road, high power diesel

generators (DG), and marine applications [21]. Use of methanol practically started recently in large-bore marine engines for commercial operations, when RoPax ferry 'Stena Germanica' was converted to operate on methanol [22]. Methanol production plants are being setup globally at feverish pace in order to meet surging demands. Mitsubishi led consortium pledged to invest US\$ 1 billion in Caribbean Gas Chemical Ltd. (CGCL) for setting up methanol-DME plant in Trinidad and Tobago recently, with one million ton methanol production capacity, in addition to 20,000 tons DME production capacity [23].

Three different approaches can be adopted for introduction of methanol in CI engines. In the first approach, methanol-diesel blend can be injected using a single injector into each cylinder. Use of a single injector for injecting diesel-methanol blend is a major advantage of this method. However, this method limits the quantity of methanol injected into CI engine because phase separation of methanol and diesel occurs, if methanol content is >10% (v/v) [6]. Several researchers have investigated CI engines fuelled with methanol-diesel blends, where maximum methanol concentration in test fuel was >10% (v/v) [24–28]. Some researchers used methanol as an additive in biodiesel-diesel blends [29–33]. Engine operational problems were observed with higher concentration methanol-diesel blends due to poor miscibility of methanol with diesel, leading to phase separation. An emulsifier can be used to overcome this issue, hence higher blending of methanol in diesel can be explored. Several researchers reported using dodecanol and a mixture of butanol (*iso*-butanol and *n*-butanol) and oleic acid as promising emulsifier solution to stabilize methanol-diesel blends [34–36]. The second approach involved methanol introduction in the intake port using port fuel injection (PFI), and direct injection of diesel into the engine combustion chamber. Several researchers have assessed this approach since it provides flexibility to use higher energy contribution from methanol to power the CI engines [37–42]. Compression ratio enhancement and intake air heating were the most commonly used approaches to avoid inferior ignition characteristics, which generally arose due to lower cetane number of methanol, and its condensation in the intake port [43–45]. In the third approach, methanol was introduced in the CI engine combustion chamber using high-pressure direct injection (HPDI) system, along with pilot injection of diesel. Diesel pilot injection initiates the combustion. In this approach also, diesel pilot is used for initiating the in-cylinder combustion first, followed by methanol injection into the burning diesel pilot flames. This approach offers an opportunity to use methanol as bulk fuel in the existing diesel engines, especially large-bore engines such as the ones used in locomotives and marine transport. This approach can be implemented in two different ways in the large-bore CI engines. First method could be installing two separate injectors for introduction of methanol and diesel, however this requires extensive modifications in the engine cylinder head. This method has design constraints because it requires additional space in the already crowded engine cylinder head to install an additional injector for methanol injection, which is quite challenging and also compromises the structural integrity of the cylinder head. This method was rarely studied and there are limited investigations reported in the open literature [46–48]. However, this method offers flexibility to handle the fuel injection timings, rate shaping, and quantity of fuel injected more precisely than other methods. First method is to develop and use a co-axial injector, which can inject two fuels simultaneously, using two separate fuel lines having independent controls in a single injector housing. Both these methods warrant use of two separate fuel tanks and two independent control units [49]. Wartsila used a co-axial injector in a medium-speed engine for marine applications [50]. Injectors used had a central diesel nozzle to inject diesel and three methanol nozzles positioned symmetrically around the diesel nozzle to inject methanol, within a common injector housing.

Methanol introduction techniques, which avoid phase separation of methanol and diesel, are obviously superior than developing methanol powered CI engines. Therefore, researchers are investigating PFI and HPDI techniques, where most energy released would be contributed by

the low-reactivity fuel 'methanol', and the high reactivity fuel 'diesel' would act merely as an ignition source [51–54]. Both these techniques provide distinct fuel introduction routes to adapt methanol in large-bore engines that would reduce their environmental impact, in addition to providing robust engine operation, in order to produce similar/ higher power density than diesel-fuelled base engines [55–57]. Limited research has been reported for the assessment of these techniques for methanol introduction in large-bore engines. This study is therefore aimed at assessing the technical feasibility of HPDI technique for methanol fueling in diesel locomotive engine using co-axial injectors. IR employs two types of diesel locomotives in its fleet. 2-stroke diesel engine technology originally procured from EMD, USA in 1990's; and 4-stroke diesel engine technology originally procured from ALCO, USA in 1950's. Both these locomotive engines have undergone significant changes and evolution in last several decades in RDSO, Lucknow (India) and have been upgraded quite significantly. ALCO design locomotive engine (ALCO-251) was selected for this feasibility assessment using 1-D simulations. Simulation is an economical and quick approach for evaluation of alternative fuels, since it provides flexibility in studying its influence on engine performance without conducting experiments using very expensive locomotive engine test-cells [58]. GT-Power is a leading simulation tool developed by Gamma Technologies, for simulating the real engine combustion conditions by simulating the gas exchange phenomena. GT-Power software has been used in this study for making a 1-D model of ALCO-251 locomotive engine. Primary objective of this study was to find optimum dimensions of the co-axial injector based on similar/ enhanced locomotive engine performance, emissions and combustion characteristics.

## 2. Methodology and computational setup

In this study, HPDI of methanol with pilot injection of diesel was chosen for modelling and computational analyses. This approach chosen for the study was based on experimental studies. Experiments performed at Engine Research Laboratory (ERL), IIT Kanpur on lower methanol-diesel blends indicated that methanol and diesel have poor miscibility and it was not possible to power a locomotive engine with 10% (v/v) methanol blended diesel. In addition, PFI technique was also investigated, where methanol was injected in the intake port to form a homogeneous charge. However, at low engine speeds, fuel-air mixture becomes very lean for the locomotive engine. It becomes difficult to ignite the fuel-air mixture under these conditions because the mixture strength goes outside the flammability limits. This technique also suffers from the issue of very high cold-start emissions. Furthermore, diesel locomotive duty-cycle was similar to urban start-and-stop duty-cycle. Port injection of methanol would have led to only nominal displacement of diesel. Hence for this study, preparation of model was followed by model validation using experimental data, which was collected from the ALCO-251 test engine at RDSO, Lucknow. Technical specifications of the locomotive test engine system are shown in Table 1.

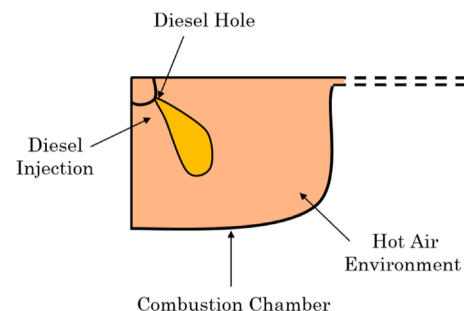
In Fig. 1, schematic representation of HPDI of (i) diesel, and (ii) methanol with pilot diesel is given. Co-axial injector is to be designed for a targeted diesel displacement (on energy basis) of 90% by methanol.

Locomotive engine works in eight notches. Notching up the engine leads to increase in engine speed and power almost linearly. Eight different engine speeds at different notches are 350 rpm (1<sup>st</sup> Notch), 450 rpm (2<sup>nd</sup> Notch), 550 rpm (3<sup>rd</sup> Notch), 650 rpm (4<sup>th</sup> Notch), 750 rpm (5<sup>th</sup> Notch), 850 rpm (6<sup>th</sup> Notch), 950 rpm (7<sup>th</sup> Notch), 1050 rpm (8<sup>th</sup> Notch). GT Power software was used to prepare 1-D model for ALCO-251 locomotive engine. In GT-Power, for creating the base model of locomotive engine, various templates were used to define different parameters associated with various engine components such as combustion chamber, injectors, valves, flow object, compressor, and turbine. Sequence of input parameters for each associated component are explained in Fig. 2.

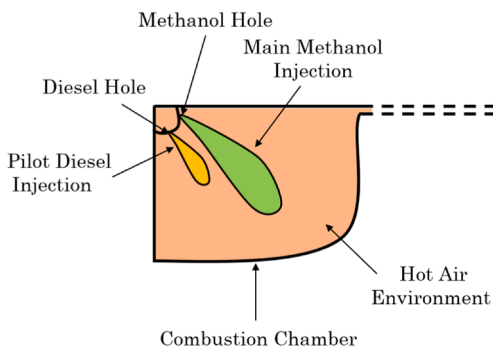
In addition, initial conditions were required as input to initialize

**Table 1**  
Technical specifications of the test engine and injector.

| Parameters               | Specifications   |
|--------------------------|--|
| Engine specifications    |  |
| Engine Type              | DLW built ALCO 251-B engine, 4-Stroke                  |
| No. of Cylinders         | 16   |
| Configuration            | 'V'  |
| Compression Ratio        | 11.75  |
| Bore × Stroke (m × m)    | 0.2286 × 0.2667  |
| Firing Order             | 1R 1L, 4R 4L, 7R 7L, 6R 6L, 8R 8L, 5R 5L, 2R 2L, 3R 3L |
| Turbocharger             | One per engine   |
| After-cooler             | Single, water-cooled                                   |
| Brake Power (kW)         | 2311   |
| Engine speed (max.)      | 1050 rpm   |
| Injector specifications  |  |
| Number of nozzle holes   | 9  |
| Hole diameter (mm)       | 0.35   |
| Spray angle              | 157 deg  |
| Make                     | Bosch  |
| Type                     | Mechanical   |
| Injection Pressure (bar) | 1050 at 8 <sup>th</sup> Notch                          |



(a) HPDI of diesel using conventional injector



(b) HPDI of methanol along and pilot injection of diesel using co-axial injector

Fig. 1. Fuel introduction strategies.

various components. Initial conditions, mostly observed in locomotive engine experiments, are listed in Table 2.

GT-Power software has two domains: GT-Integrated Simulation Environment (GT-JSE) and GT-Post Processing Tool (GT-Post). The first one is used for building the model and to assign simulation parameters. The second is used for post-processing of data, where plot-processing feature is also available. In this study, two injectors in a single co-axial injector body are modeled to assess its feasibility. Detailed steps followed in this study are shown in the flow-chart (Fig. 3).

Sixteen-cylinder locomotive engine model is shown in Fig. 4.

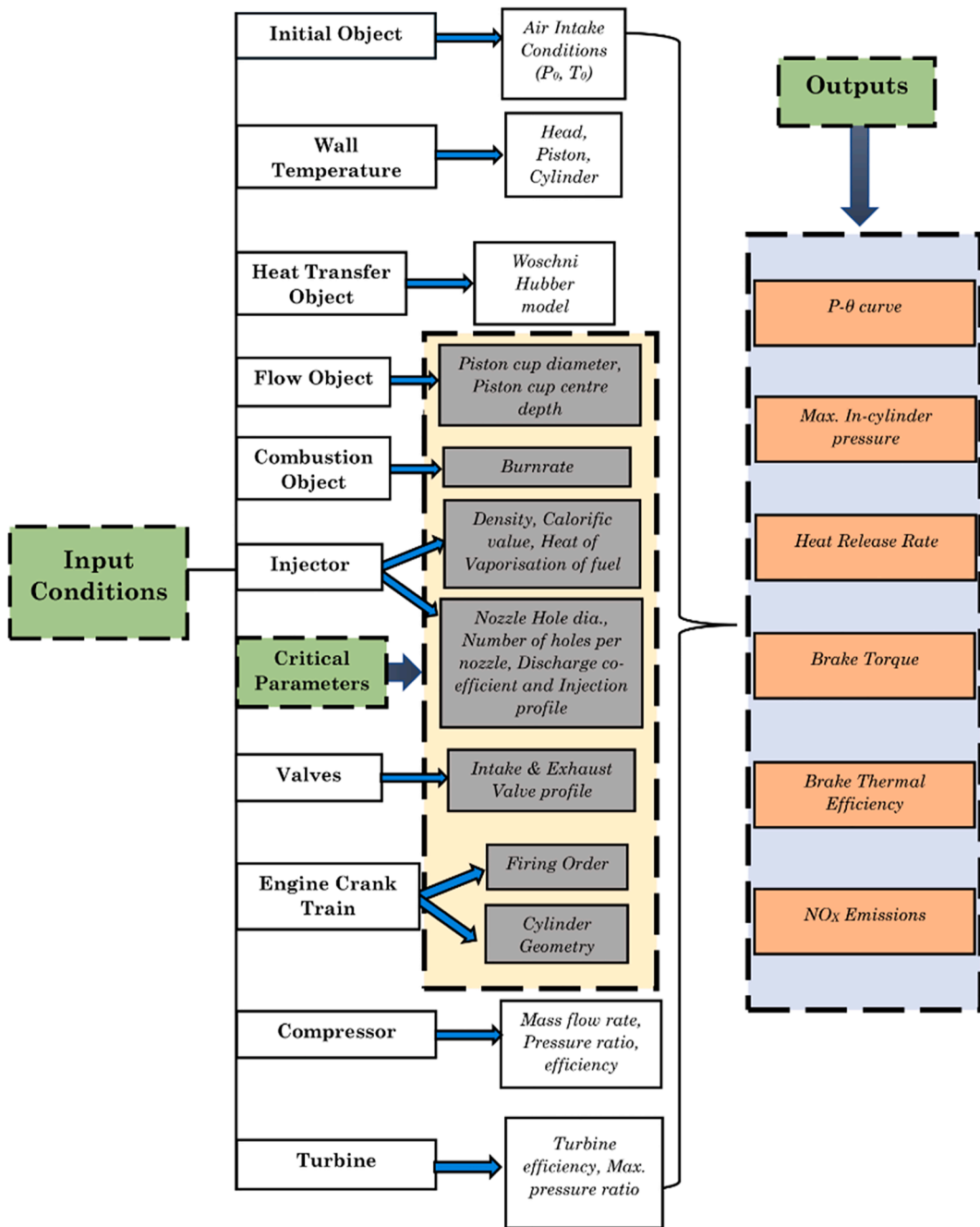


Fig. 2. Model flow-chart explaining different objects and associated parameters required for 1-D model preparation.

Table 2  
Initial operating conditions for the base-model.

| Parameters                        | Unit | Value |
|-----------------------------------|------|-------|
| Initial pressure (Environment)    | bar  | 1     |
| Initial temperature (Environment) | K    | 300   |
| Head temperature                  | K    | 550   |
| Piston temperature                | K    | 525   |
| Cylinder temperature              | K    | 500   |

Different colour mapping is used to differentiate between various objects considered in the model. Prediction of heat exchange processes plays a vital role in validation of 1-D model with the experimental data. For this, GT-Power offers several heat transfer models such as WoschniClassic, WoschniGT, WoschniSwirl, WoschniHuber, Hohenberg etc.,

for simulating the heat exchange processes. For the base model validation, WoschniHuber model was used, since it uses the in-cylinder flow model and swirl number from the central region for superior accuracy of heat transfer prediction. The convective heat transfer coefficient is defined as follows: [59]

$$h_c = \frac{3.26p^{0.8}w^{0.8}}{B^{0.2}T^{0.53}} \quad (1.1)$$

where  $h_c$  = Convective heat transfer coefficient ( $\text{W}/\text{m}^2\text{.K}$ ),  $B$  = Cylinder bore (m),  $p$  = Cylinder pressure (kPa),  $T$  = Cylinder Temperature (K),  $w$  = Average cylinder gas velocity (m/s), which is defined as follows: [60]

$$w = \max(ww, wh) \quad (1.2)$$

where  $ww$  = Conventional Woschni model average in the cylinder,  $wh$

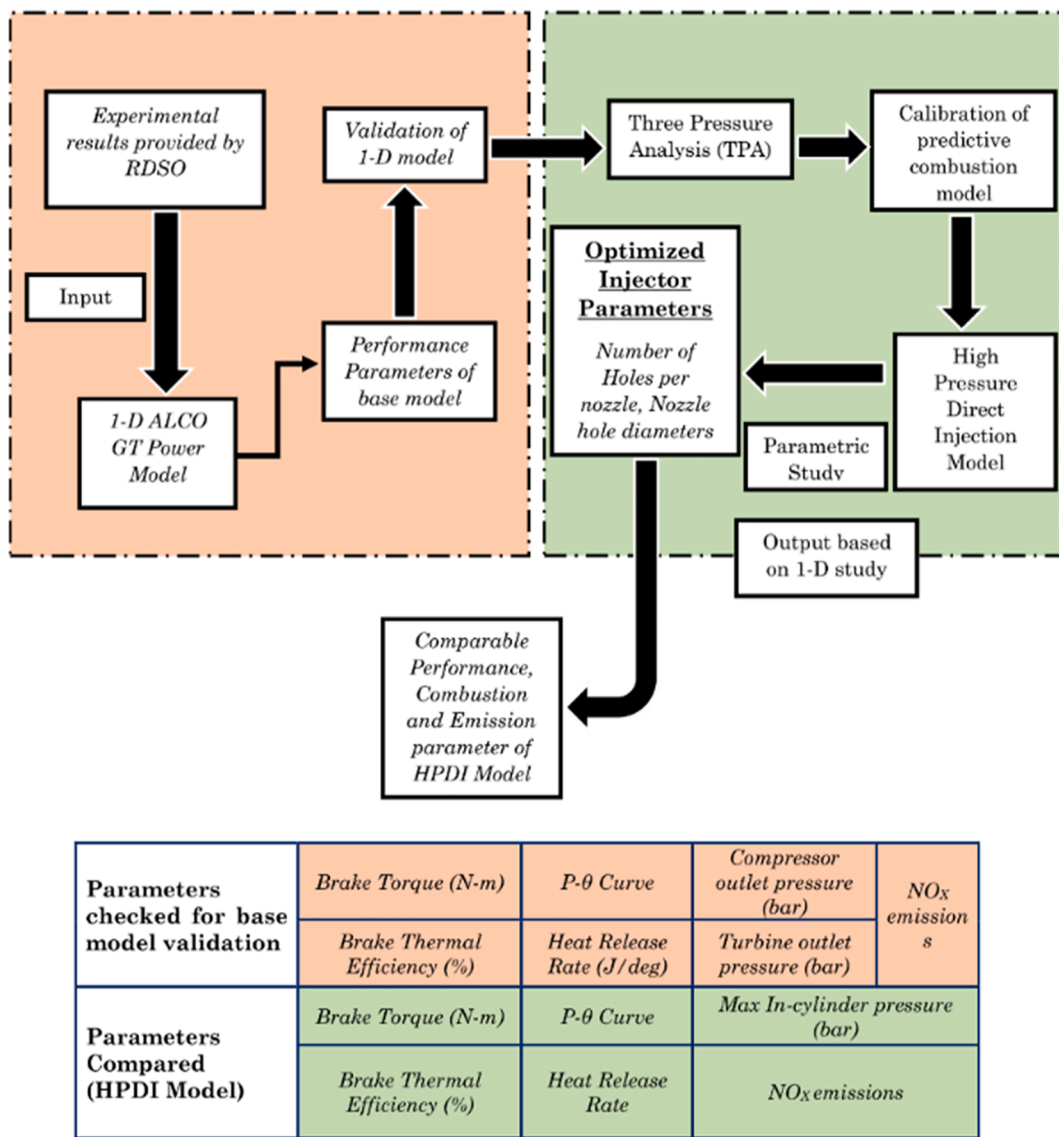


Fig. 3. Schematic of the modeling procedure.

= Huber average in the cylinder gas velocity, which is defined as follows: [60]

$$wh = C_1 S_p \left( 1 + 2 \left( \frac{V_{TDC}}{V} \right)^2 (\max(IMEP, 1))^{-0.2} \right) \quad (1.3)$$

where IMEP = Indicated Mean Effective Pressure (bar),  $S_p$  = Mean piston speed (m/s),  $V$  = Volume ( $m^3$ ),  $V_{TDC}$  = Volume at top dead centre ( $m^3$ ), and  $C_1$  = Constant as mentioned in Table 3.

During the model preparation, combustion model was needed to be defined by the user, where the burn-rate and start of combustion (SoC) were required as inputs. Using the validated model, HPDI model with co-axial injector was prepared, where methanol was injected directly into the cylinder, along with pilot injection of diesel. In this model, one of the main bottlenecks was the burn-rate. It was required as an input parameter for the engine performance calculations. The burn-rate signifies fuel consumption during in-cylinder combustion process. Experimental data for HPDI model with co-axial injector concept for methanol utilization in the locomotive engine was not available in the open literature. Following procedural steps were used for HPDI model development with co-axial injector.

#### Step 1: Three Pressure Analysis (TPA)

TPA model was used for burn-rate prediction from the measured in-cylinder pressure data of diesel-fuelled locomotive engine. It is a reverse run method, where diesel cylinder pressure history was given as an input and burn-rate was the output. The flow characteristics of the model should be accurate to get precise results from the TPA analysis. This condition can be assured by isolating the model for one cylinder along with its associated valves and ports. In TPA analysis, combustion object was not given as an input.

#### Step 2: Calibration of Predictive Combustion Model

Predictive combustion model was used for modelling the physics of combustion process to predict the burn-rate in the engine combustion chamber. In reality, predictive combustion model includes assumptions since it is based on three pressures only. Therefore, model requires calibration for the best match of simulated combustion process with that of the experimental data of combustion. GT power finds four DIPulse attributes. These attributes are such that the best match is defined between measured and predictive burn-rates. These attributes are entrainment rate multiplier, ignition delay multiplier, premixed

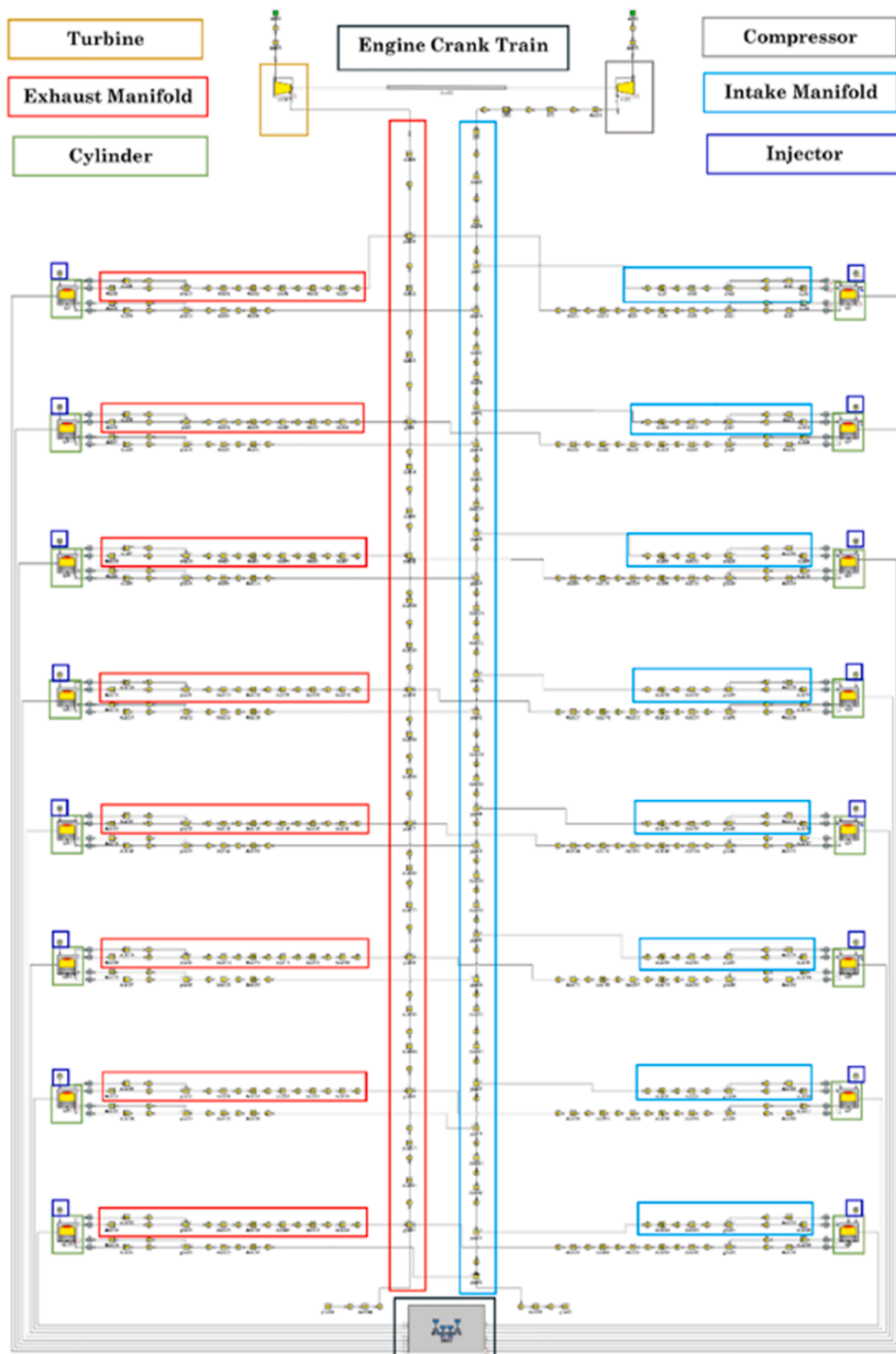


Fig. 4. Base-model for 16-cylinder locomotive engine using GT-Power.

**Table 3**  
Value of constant  $C_1$  used in prediction of heat transfer [60].

| $C_1$                           | Process            |
|---------------------------------|--------------------|
| During cylinder gas exchange    | $6.18 + 0.417 S_w$ |
| During compression              | $2.28 + 0.308 S_w$ |
| During combustion and expansion | $2.28 + 0.308 S_w$ |

where;  $S_w$  = Swirl number of centre regions.

combustion rate multiplier, and diffusion combustion rate multiplier. Different attributes are briefly explained, which are used in GT-Power for various multiplier calculations.

#### Step 3: HPDI of Methanol with Pilot Diesel Injection Model

For displacing 90% diesel energy by methanol, HPDI of methanol with diesel pilot injection model was prepared, which used a co-axial injector for injecting methanol and diesel pilot in the cylinder sequentially (Fig. 5).

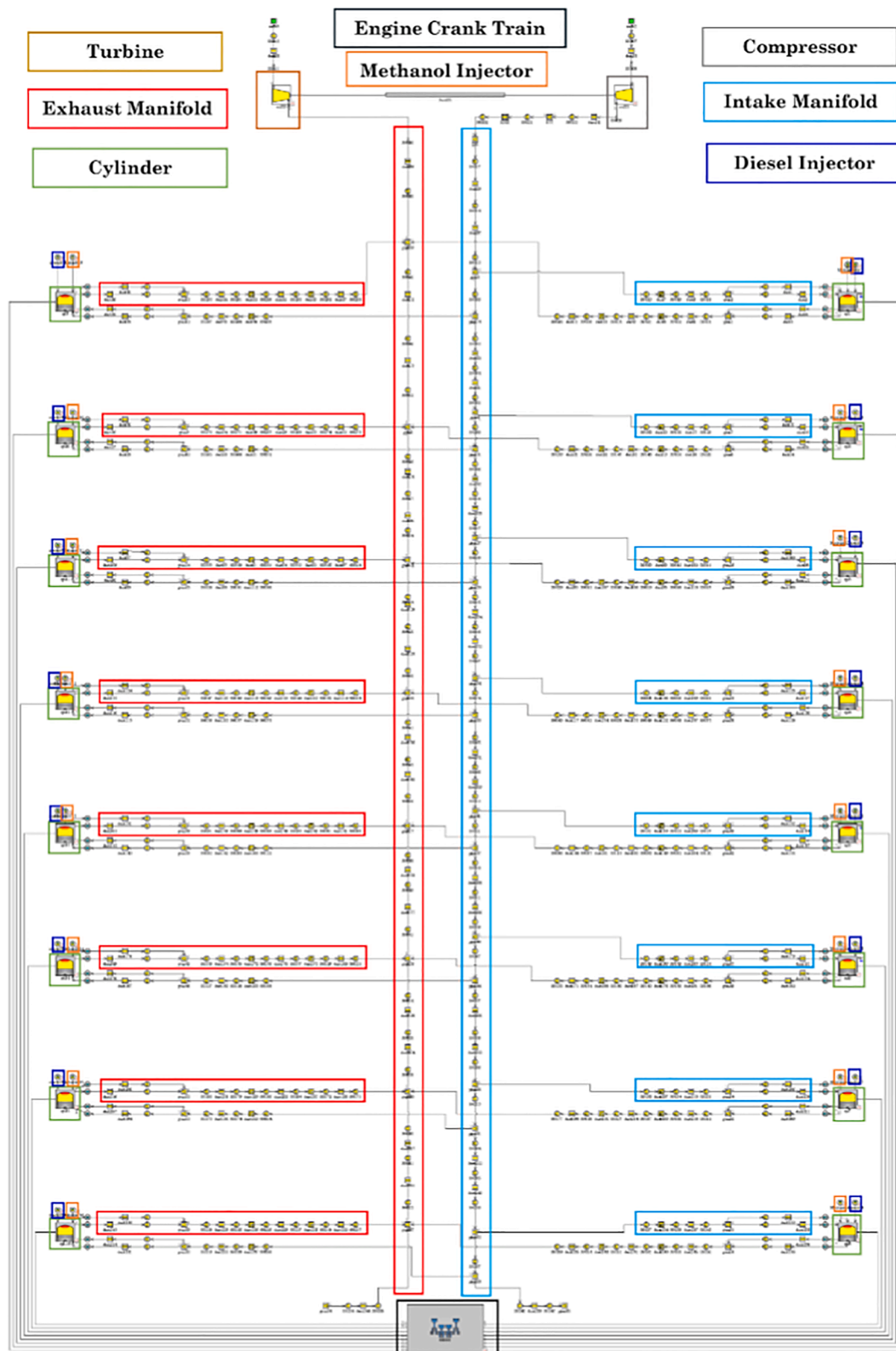


Fig. 5. HPDI of methanol with pilot diesel injection model in GT-Power.

Co-axial injector was represented as two injectors in the model, in order to assess the capability of this conceptual fuel injection system design. Methanol was selected as one of the two fuels along with diesel from the GT-Power library, and the input parameters taken from the library were as given in Table 4.

Since 90% diesel displacement by methanol is on energy basis was

targetted, methanol and diesel quantities were calculated and given as input to the model. Injected fuel quantity along with their injection pressures for both, the base model, and the HPDI of methanol with pilot diesel injection model are shown in Fig. 6. For HPDI of methanol with pilot diesel injection model, EngCylCombDIPulse (Direct-Injection-Diesel-Multi-Pulse) combustion model was used. It predicts the

**Table 4**  
Parameters taken from GT-power library for the two test fuels.

| Parameter                          | Diesel  | Methanol |
|------------------------------------|---------|----------|
| Carbon atoms per molecule          | 15      | 1        |
| Hydrogen atoms per molecule        | 25.05   | 4        |
| Oxygen atoms per molecule          | 0       | 1        |
| Stoichiometric air-fuel ratio      | 14.5:1  | 6.42:1   |
| Density (Kg/m <sup>3</sup> )       | 830     | 792      |
| Lower heating value (MJ/kg)        | 42.8    | 21.1     |
| Critical temperature (K)           | 569.4   | 513      |
| Critical pressure (bar)            | 24.6    | 79.5     |
| Absolute entropy at 298 K (J/kg-K) | 3445.47 | 7484.33  |

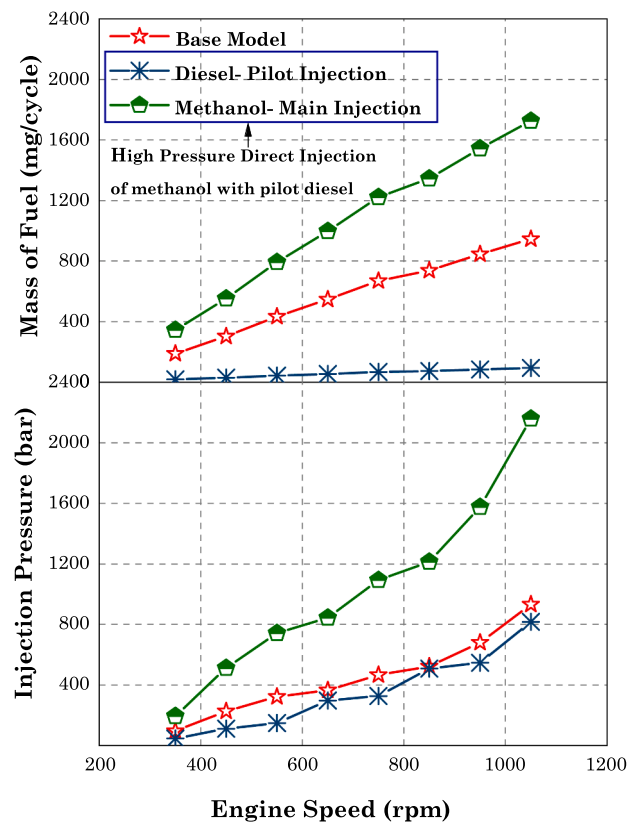


**Fig. 6.** (a) Fuel quantity injected in one engine cycle, and (b) Fuel injection pressure for base model and HPDI of methanol with pilot diesel injection model.

combustion rate in accordance with single or multiple injection events. Basic approach for this model is to track the fuel droplets as an injection event occurs, its evaporation due to high in-cylinder temperature environment, and finally the mixture formation with surrounding gases, followed by combustion. These predictive model calculations were done in three different zones: (i) main unburned zone, (ii) spray unburned zone, and (iii) spray burned zone. In this combustion model, an optimized entrainment rate multiplier, ignition delay multiplier, premixed combustion rate multiplier, and diffusion combustion rate multiplier were given as input, as mentioned in the Step 2.

Start of injection (SoI) timing, number of holes and holes diameter of diesel injector nozzle and methanol injector nozzle for 'HPDI of methanol with diesel pilot injection model' were found by optimization. Optimization is the process where systematic changes were done in the input variables (factors) for maximizing or minimizing model's outputs. It is an automated process with following steps: it (i) iteratively sets the input variables, (ii) runs the model, (iii) evaluates the model outputs, and (iv) changes the inputs again for optimization of objectives. GT-Power provides the facility of Integrated Design Optimizer that

accommodates the sweep factors, for which a single optimized value will be found for current active cases. Steps followed for the optimization procedure are as follows:

Multiple objectives (Pareto) selected were to maximize the engine performance, and to minimize the emissions. Thus, design optimizer was setup with two independent factors, and three sweep factors with objective of brake torque, and brake power maximization along with NOx minimization.

SoI of diesel injector and methanol injector were selected as independent factors. Also, diesel nozzle hole diameter and number of holes, methanol nozzle hole diameter and number of holes were selected as sweep factors.

Design optimizer was run such that optimized injector parameters of both injectors and SoI timings for both fuel injection for HPDI of methanol with diesel pilot model were determined, as shown in Tables 5 and 6 respectively.

The reason for injecting 10% energy by diesel in 'HPDI of methanol with pilot diesel injection model' was to use diesel for initiation of combustion. During optimization of SoI timing for methanol, injection event was found to be relatively retarded such that diesel injection took place earlier than the methanol injection, and it initiated the combustion in the engine cylinder before the methanol was injected. The proposed co-axial injector for methanol induction along with pilot diesel injection and its optimum dimensions are illustrated in Fig. 7.

### 3. Results and discussion

In this section, first the base model for diesel was validated using the experimental results, and then the engine performance, emissions, and combustion parameters of HPDI of methanol with pilot diesel injection model were compared with that of the base model, in order to see whether large energy displacement of diesel by methanol would lead to identical locomotive engine performance or not?

#### 3.1. Base model validation

1-D base model prepared using GT-Power was validated using the experimental data provided by RDSO. Variations in the engine performance, emissions and combustion are discussed in this section. Various parameters such as P-θ diagram, heat release rate (HRR), brake torque, brake thermal efficiency, maximum in-cylinder pressure, NOx emissions, turbine outlet pressure, compressor outlet pressure etc. were considered for base model validation using the experimental data from the ALCO-251 locomotive.

##### 3.1.1. P-θ diagram and heat release rate

1-D base model for ALCO 251 locomotive was validated at four notches (8<sup>th</sup> Notch, 7<sup>th</sup> Notch, 6<sup>th</sup> Notch and 5<sup>th</sup> Notch), while considering appropriate matching of P-θ and HRR curves with the measured experimental data (Fig. 8). P-θ curves at all these notches followed the trends at start of combustion and the expansion strokes. However, there were some differences in the peak pressures produced, assuming that experiments were performed after the thermal stabilization and data

**Table 5**

Injector dimensions for a single injector (only diesel) and co-axial injector (HPDI of methanol with pilot diesel injection).

| Injector parameters    | Diesel injector (Base Model) |                   | Co-Axial Injector (HPDI of methanol with pilot diesel injection model) |                   |
|------------------------|------------------------------|-------------------|--|-------------------|
|                        | Diesel injector              | Methanol injector | Diesel injector  | Methanol injector |
| Hole diameter (mm)     | 0.35                         |                   | 0.486  | 0.544             |
| Number of nozzle holes | 9                            |                   | 3  | 5                 |

**Table 6**  
Start of injection timings.

| Model        | Injector | Engine speed (Erpm) |         |         |         |         |         |         |         |    |
|--------------|----------|---------------------|---------|---------|---------|---------|---------|---------|---------|----|
|              |          | 1050 rpm            | 950 rpm | 850 rpm | 750 rpm | 650 rpm | 550 rpm | 450 rpm | 350 rpm |    |
| SOI (degree) | BM       | D                   | -15     | -16     | -18     | -22     | -14     | -12     | -10     | -6 |
|              | DM       | D                   | -16     | -14     | -17     | -22     | -14     | -10     | -9      | -7 |
|              | M        | M                   | -14     | -13     | -14     | -17     | -11     | -7      | -6      | -3 |

D: Diesel, M: Methanol, BM: Base model, DM: HPDI of methanol with pilot diesel injection model.

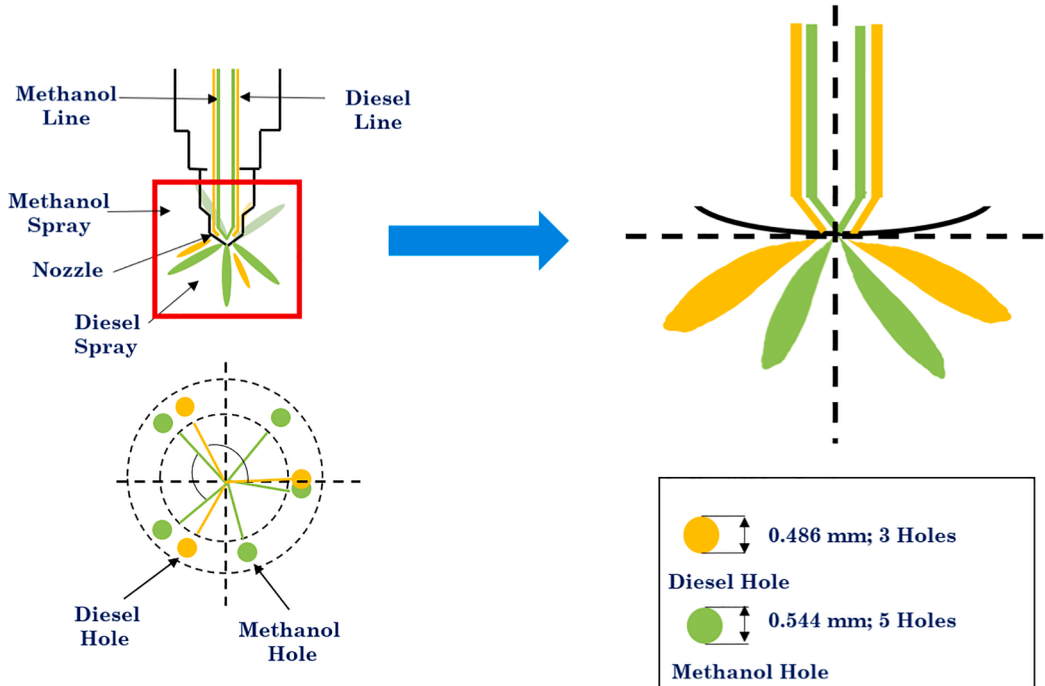


**Fig. 7.** Illustration of proposed co-axial injector dimensions for adapting methanol and pilot diesel injection in a locomotive engine.

captured were accurate. The differences in both the experimental and simulated  $P_{max}$  are shown in Fig. 9 (a) at all notches. This difference were mainly contributed by the idealization and assumptions made, while predicting different parameters. The highest differences in the in-cylinder pressures between the experimental and simulation results were found at the 7<sup>th</sup> Notch.

Simulation results matched well but were slightly lower than the experimental results at all notches. The minor variations between the peak in-cylinder pressure between the simulation and experimental results were because engine combustion remained quite complex and not well understood phenomena and empirical relations used in 1-D model were not sophisticated enough to consider numerous factors, that affect the combustion process as shown in Fig. 9(a). Moreover, HRR at different notches was considered as an important factor for validation of 1-D model because model predicted accurate results to emulate heat released during the combustion process. Shapes of HRR of both experimental and simulation results were similar but minor differences were there. These differences can be attributed to noise in the measurement of the experimental data and/ or incorrect data filtering. Also, it is possible that heat exchange between gases and cylinder walls was not modelled accurately in the 1-D simulation model. These deviations between the experimental and simulation results in both  $P$ - $\theta$  and HRR curves were within acceptable range. Therefore, the model was considered validated and could be used for assessing the engine performance, emissions and combustion related parameters.

### 3.1.2. Brake torque (BT)

The variations of BT in the experimental and simulation results is shown in Fig. 9 (b). Maximum BTs in the experimental and simulated results at 8<sup>th</sup> notch were 20,702 Nm and 20,426 Nm respectively. Simulated results were marginally higher than the experimental results at all notches except first, second and sixth notches. Experimented brake torques at eighth, seventh, fifth, fourth, and third notches were 20,702, 18,406, 13,298, 10259, 7813 Nm, whereas simulated brake torques were 20,426, 18319, 12938, 10060, and 7574 Nm respectively. Slight variations was observed between the experimental and simulations because WoschniHuber model used for heat transfer prediction and calculations. Heat transfer based on empirical relationship do not account for transient variations in the related parameters such as intake air temperature, engine surface temperature etc.

### 3.1.3. Brake thermal efficiency (BTE)

1-D model also gives the brake thermal efficiency (BTE) as an output. The variations in both the experimental and simulated BTE results are shown in Fig. 9(c). Higest differences in the BTE between the experimental and simulation results were observed at the eighth notch, which were 40.82 and 39.9%, respectively. The model simulated slightly lower BTE compared to the experimental results of BTE at all notches, except the second notch. Experimental BTE at the second notch was 31.64%, whereas simulated BTE was 32%. Maximum difference in the values of experimental and simulated BTEs were observed at the first notch (~5% of the experimental value).

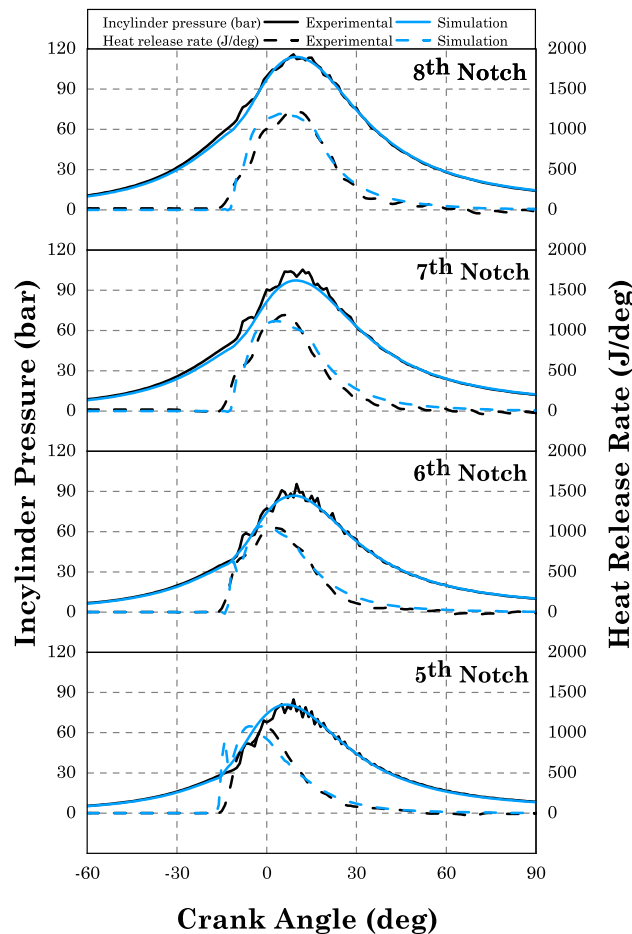


**Fig. 8.** In-cylinder pressure and HRR (J/deg) vs crank angle at (a) 8<sup>th</sup> Notch (1050 rpm) (b) 7<sup>th</sup> Notch (950 rpm), (c) 6<sup>th</sup> Notch (850 rpm), and (d) 5<sup>th</sup> Notch (750 rpm).

### 3.1.4. NO<sub>x</sub> emissions

GT-Suite combustion models are capable of calculating the NO<sub>x</sub> emissions using Extended Zeldovich mechanism. In NO<sub>x</sub> emission modelling, results are quite sensitive for trapped in-cylinder mass, combustion rate and air-fuel ratio hence simulation results depend on the values given as inputs. NO<sub>x</sub> is also sensitive to the in-cylinder temperature, therefore 'two-temp' model was used during combustion modelling because single-zone temperature calculations were not enough to capture the in-cylinder temperature. NO<sub>x</sub> validation was done using the experimental data. The differences between the experimental and simulated results are shown in Fig. 9(d). The highest experimental and simulated NO<sub>x</sub> emissions were observed at the 3<sup>rd</sup> notch and the 5<sup>th</sup> Notch respectively (1617 and 1343 ppm).

The model simulated slightly lower NO<sub>x</sub> emissions compared to experimental NO<sub>x</sub> emissions at all notches. The lowest differences between the experimental and simulated results of NO<sub>x</sub> emissions were observed at the last four notches, which were ~ 2.2% at 8<sup>th</sup> Notch, ~ 2.9% at 7<sup>th</sup> Notch, ~ 1.9% at 6<sup>th</sup> Notch and 5.2% at the 5<sup>th</sup> Notch. Other Notches exhibited higher differences between the experimental and simulation results. NO<sub>x</sub> emission calibration provided certain multipliers such as NO<sub>x</sub> calibration multiplier, and N<sub>2</sub> oxidation activation energy multiplier, which were used to predict the net rate of NO<sub>x</sub> formation and activation energy multiplier of N<sub>2</sub> oxidation rate equation. These multipliers are unique for all notches.

### 3.1.5. Turbine outlet pressure ( $P_{to}$ ) and compressor outlet pressure ( $P_{co}$ )

The model used for simulations had a turbocharging unit. Turbine

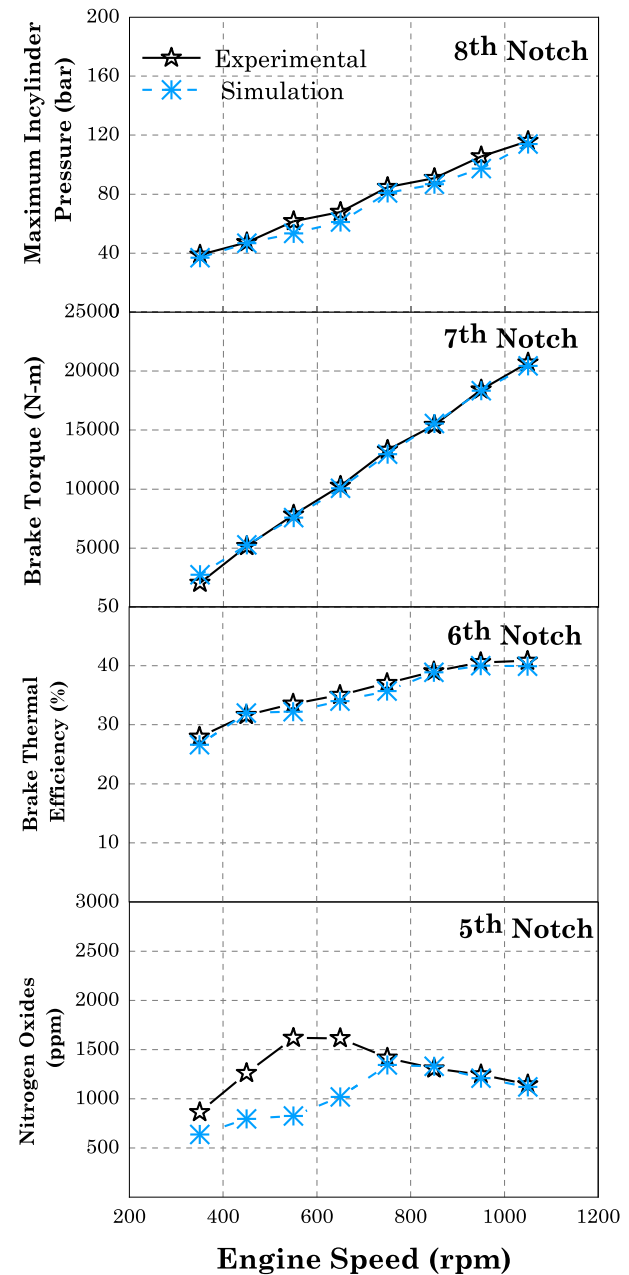


**Fig. 9.** (a) Maximum In-cylinder pressure (bar) vs Engine speed (rpm), (b) Brake Torque (N-m) vs Engine speed (rpm), (c) Brake Thermal Efficiency (%) vs Engine speed (rpm), and (d) Nitrogen Oxides (ppm) vs Engine speed (rpm) curves.

outlet pressure and compressor outlet pressure play a vital role because they have a direct impact on the engine performance parameters. The differences in experiment and simulation results for  $P_{co}$  and  $P_{to}$  are shown in Fig. 10. Highest experimental and simulated values of  $P_{co}$  were observed at the 8<sup>th</sup> notch, which were 2.6 bar and 2.4 bar respectively, as shown in Fig. 10 (a). Simulation results were slightly lower than the experimental results at all notches. Initially, at the first notch, difference between the experimental and simulated values of  $P_{co}$  was ~ 0.01%, which was the lowest difference of all notches. Highest difference between the experimental and simulated results was at the 5<sup>th</sup> notch (~11.8%).

Difference in experimental and simulated results of turbine outlet pressure is shown in Fig. 10(b). Maximum values of  $P_{to}$  from the experiments and simulations were observed at the 8<sup>th</sup> notch, which were

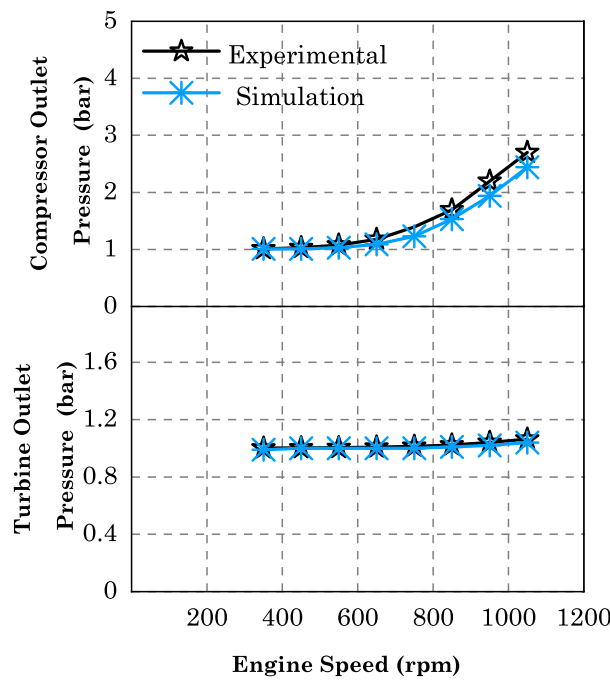


**Fig. 10.** (a) Compressor outlet pressure (bar) vs Engine Speed (rpm) (b) Turbine outlet pressure (bar) vs Engine Speed (rpm).

1.06 and 1.04 bar, respectively. Simulation model predicted the turbine outlet pressure adequately well. At the first notch, the difference between the experimental and simulated results was  $\sim 1.17\%$ , and at the 8<sup>th</sup> notch, this difference was only 2.24%.

In summary, all performance, emissions and combustion parameters were simulated quite well by the base model, and the simulated parameters could be predicted in proximity of the experimental results. Therefore, the base model was validated. This validated model can be used for introduction of methanol using HPDI technique in diesel locomotive engines, along with pilot injection of diesel, as given in section 3.2.

### 3.2. HPDI of methanol with pilot diesel injection model

The main aim of this study was to assess the feasibility of methanol fueling of locomotive engines. In this section, locomotive engine performance, emissions, and combustion characteristics of HPDI of methanol with pilot diesel injection model were compared with the results of the base-model.

#### 3.2.1. P-θ and HRR curves

Fig. 11 shows the in-cylinder pressure and HRR of the 1-D base model and HPDI of methanol with pilot diesel injection model at the 8<sup>th</sup> Notch, 7<sup>th</sup> Notch, 6<sup>th</sup> Notch, and 5<sup>th</sup> Notch of the locomotive engine. In-cylinder pressure curve shapes of HPDI of methanol with pilot diesel model were similar to the validated base model at various notches. However, HRR curve shapes of the co-axial injector model were slightly different from the base-model, which was attributed to difference in fuel injection strategy, i.e. use of diesel pilot injection in co-axial injector model to initiate combustion in the locomotive engine, where 90% fuel energy was delivered by methanol. Methanol has higher latent heat of vaporization compared to mineral diesel, and it plays a vital role in initiating the combustion. Moreover, in 1-D base model diesel burns in diffusion combustion mode, whereas in the co-axial injector model, first pilot diesel was injected into the combustion chamber (diffusion combustion), followed by methanol direct injection in the combustion chamber. Methanol fuelled co-axial injector model showed higher peak in-cylinder pressure at all notches compared to validated base model.

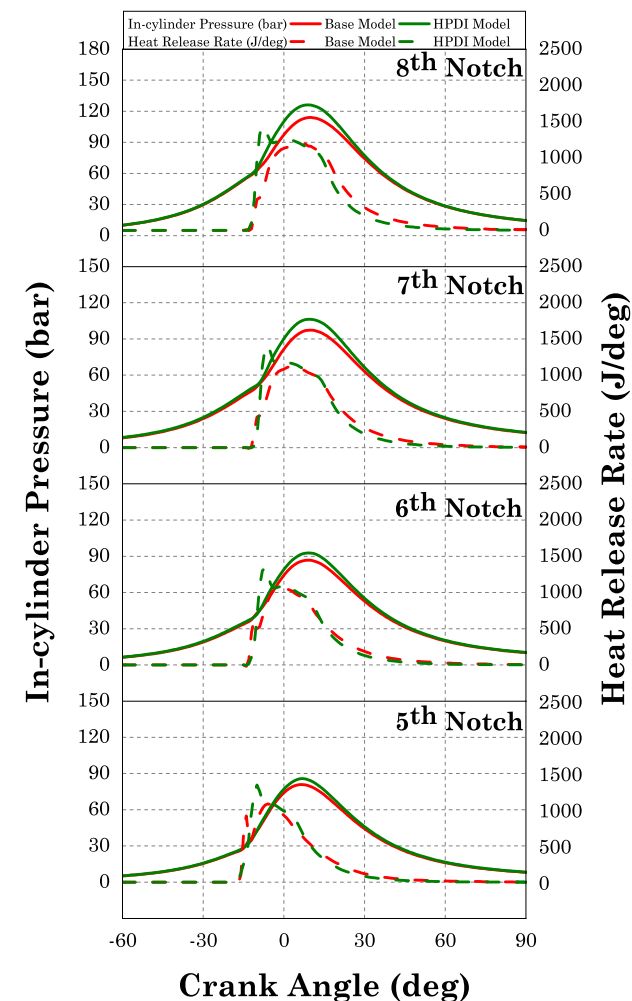


**Fig. 11.** In-cylinder pressure (bar) and HRR (J/deg) vs Crank Angle Position (deg) for (a) 8<sup>th</sup> Notch: 1050 rpm, (b) 7<sup>th</sup> Notch: 950 rpm, (c) 6<sup>th</sup> Notch: 850 rpm, and (d) 5<sup>th</sup> Notch: 750 rpm.

Peak in-cylinder pressures were 120.26, 99.70, 87.02 and 80.98 bar at 8<sup>th</sup>, 7<sup>th</sup>, 6<sup>th</sup>, and 5<sup>th</sup> notches respectively. In general, methanol fuelled co-axial injector model exhibited higher peak in-cylinder pressures compared to the validated base model at different notches.

#### 3.2.2. Maximum in-cylinder pressure ( $P_{max}$ )

Fig. 12(a) shows a comparison of HPDI of methanol with diesel pilot injection model with the validated base-model for maximum in-cylinder pressure. Maximum in-cylinder pressures for validated base-model and investigated model were observed at the 8<sup>th</sup> notch, which were 114.05 and 120.26 bar, respectively. Higher maximum in-cylinder pressure was reflected by the investigated model using co-axial injector at the 8<sup>th</sup>, 7<sup>th</sup>, and 6<sup>th</sup> notches. Methanol direct injection with diesel pilot model showed an identical trend for  $P_{max}$  at all notches, and it confirmed that methanol fuelling with diesel pilot injection could power the locomotive at all notches, similar to only diesel fuelling, and deliver improved engine combustion characteristics.

#### 3.2.3. Brake torque (BT)

Fig. 12(b) showed a comparison of HPDI of methanol with pilot diesel injection model with validated base-model for the BT. Maximum values of BTs for the validated base-model and HPDI of methanol with pilot diesel injection model were observed at the 8<sup>th</sup> notch. These were 20426.9 and 20395.8 Nm respectively. At the 1<sup>st</sup> notch, BT for base-model and HPDI of methanol with pilot diesel injection model were

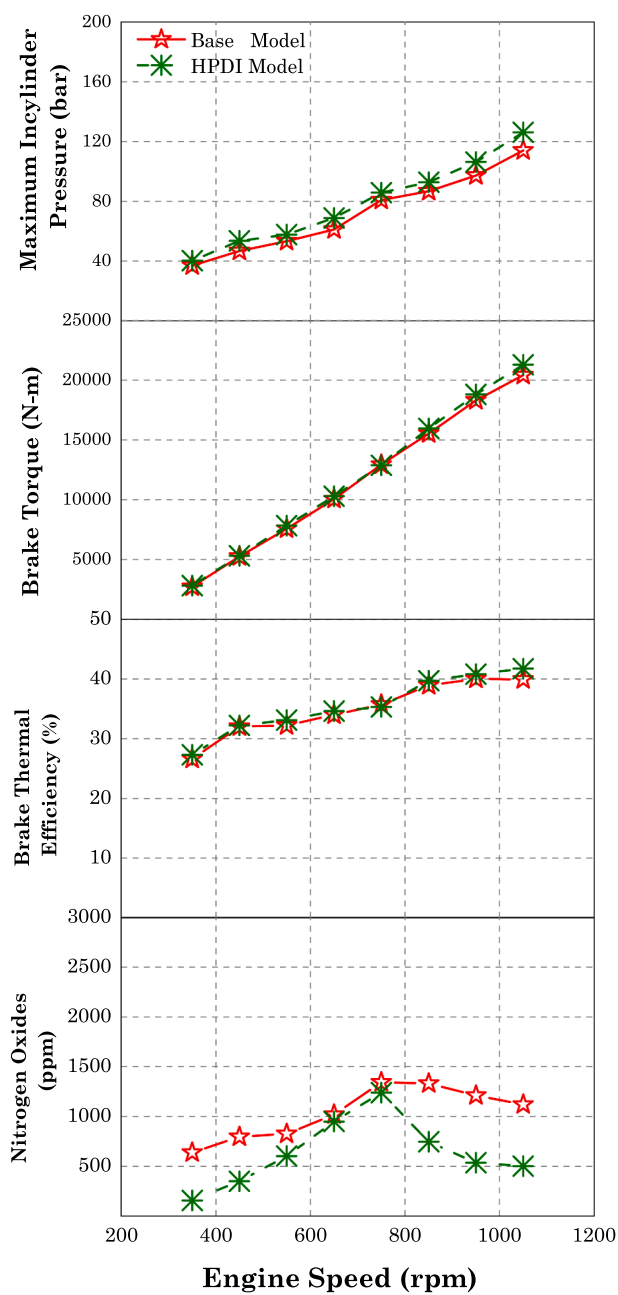


**Fig. 12.** Comparison of Direct injection of methanol with diesel pilot injection model with base-model for (a) Maximum in-cylinder pressure (bar) vs Engine speed (rpm), (b) Brake torque (Nm) vs Engine speed (rpm), (c) Brake Thermal Efficiency (%) vs Engine speed (rpm), and (d) Nitrogen Oxides (ppm) vs Engine speed (rpm).

2724.3 and 2603.1 Nm respectively. Inherent oxygen of methanol improved the combustion efficiency at all notches. It is very clear that the locomotive engine with co-axial HPDI of methanol with pilot diesel injection was able to deliver identical or better torque compared to the base-model. Methanol direct injection with diesel pilot model showed an identical trend for BT at all notches, and it confirmed that methanol fuelling with diesel pilot injection could power the locomotive at all notches similar to only diesel fuelling, while delivering improved engine performance.

#### 3.2.4. Brake thermal efficiency (BTE)

Fig. 12(c) shows a comparison of BTE for HPDI model and validated base-model. The maximum BTE observed at the 8<sup>th</sup> notch were 41.7 and

39.9% for HPDI model and base-model respectively. In general, comparable or superior BTE was observed with methanol fuelling compared to base-model at all notches. Clearly, methanol HPDI with diesel pilot injection model showed an identical trend for BTE at all notches, and it confirmed that methanol fuelling with diesel pilot injection could power the locomotive at all notches, quite similar to only diesel fuelling, while delivering improved engine performance.

#### 3.2.5. Nitrogen oxides emissions

Fig. 12(d) shows a comparison of HPDI of methanol with diesel pilot injection model with validated base-model for emissions, primarily NOx emissions. NOx is dependant on fuel oxygen concentration, peak in-cylinder temperature, and residence time of reaction at extreme in-cylinder conditions [61,62]. Methanol fuelled co-axial injector model generated lower NOx emissions at all notches compared to validated base-model. Lower NOx were formed due to methanol's relatively higher latent heat of vaporization, which reduced the peak in-cylinder temperature, thereby lowering the formation of NOx at all notches. Clearly, methanol HPDI with diesel pilot injection model showed a superior trend of lower NOx emissions at all notches, and it confirmed that methanol fuelling with diesel pilot injection could power the locomotive at all notches, quite similar to only diesel fuelling, while delivering lower emissions.

## 4. Conclusions

In this investigation, high pressure co-axial direct injection system was investigated for methanol fueling using 1-D simulation approach. Diesel fueled locomotive engine was operated at different engine speeds at different notches and collected data were provided for this simulation study. 1-D Model of ALCO-251 locomotive engine was prepared using GT-Power and integrated with available empirical models of heat transfer, combustion, and emissions. For this study, WoschniHuber model was used to calculate the heat transfer interactions. This base-model was validated using experimental data from RDSO. The differences between the experimental and simulation results for engine performance, emissions and combustion characteristics were within an acceptable range. After validating the base-model using the experimental data, high pressure direct injection of Methanol with pilot diesel injection model was prepared for 90% diesel energy displacement by methanol. A co-axial injector consisting of two injectors in a single injector body was used to assess its capabilities for methanol injection. SoI timing of methanol injector was retarded to explore diesel pilot injection, which was followed by HPDI of methanol in the engine cylinder. Results indicated that upon displacing 90% diesel energy by methanol, locomotive engine generated similar power output as that of diesel only fuelling at all notches. From this 1-D simulation study, optimum injector dimensions of co-axial injector were found to be: (i) 0.486 mm nozzle hole diameter with 3 holes for diesel injection, and (ii) 0.544 mm nozzle hole diameter with 5 holes for methanol injection. However, an experimental study after developing the co-axial injector having the predicted dimensions is required before practical implementation of this strategy on a large-scale in locomotives. In summary, methanol can be used in locomotive engines as a traction fuel. Co-axial injector design opens new avenues for introduction of higher quantities of methanol for large displacement of mineral diesel. Simulation results showed that ALCO-251 locomotive exhibited superior performance, emissions, and combustion characteristics, which were better base locomotive engine with diesel only fueling. This work opens up new avenues for utilizing Methanol and other alternative fuels in locomotive engines, which do not mix well with conventional fuels.

## 5. Limitations and future scope

Predictive combustion model is used in HPDI of methanol with pilot diesel injection model for combustion of methanol and diesel. Prediction

works on various assumptions and gives slightly different results than the actual experimental results. The variations are because of the following factors:

Physico-chemical properties of fuel were directly taken from the GT library. In reality, fuel properties could be slightly different.

This work is based on 1-D simulation only. It requires further investigations using 3-D simulations, followed by actual engine experiments on reduced number of optimized configurations emerging from the simulation studies.

Co-axial injector needs to be manufactured for the experimental validation of performance, emissions and combustion characteristics.

#### CRediT authorship contribution statement

**Dhananjay Kumar:** Data curation, Formal analysis, Investigation, Validation, Writing - original draft. **Hardikk Valera:** Data curation, Formal analysis, Investigation, Validation, Writing - original draft. **Anirudh Gautam:** data supply for model validation. **Avinash Kumar Agarwal:** Conceptualization, Methodology, Project administration, Resources, Supervision, Writing - review & editing.

#### Declaration of Competing Interest

The authors declare the following financial interests/personal relationships which may be considered as potential competing interests: 1. Prof. Ashwani Gupta, Department of Mechanical Engineering, University of Maryland, USA; 2. Prof. S K Aggarwal, Mechanical Engineering Department, University of Illinois, Chicago, USA.

#### Acknowledgments

The authors would like to acknowledge the Department of Science and Technology (DST), Government of India (Sanction Number TMD/CERI/MDME/2017/003 (G) dated 11-12-2017) for generous funding support for procurement of simulation softwares and high-performance computational infrastructure and other equipment as required for this study. The authors also would like to acknowledge Mr. Pavan Chandra and Mr. Ramnik Singh from GT-Suite (India) for their constant support in simulating and model preparations for this project.

#### References

- [1] Indian Railway Industry Report. Available From: <https://www.ibef.org/industry/indian-railways.aspx> accessed on 1st September 2020.
- [2] Indian Railways Facts & Figures (2016-17). Available From: [http://www.indianrailways.gov.in/railwayboard/uploads/directorate/stat\\_econ/IRSP\\_2016-17/Facts\\_Figure/Fact\\_Figures%20English%202016-17.pdf](http://www.indianrailways.gov.in/railwayboard/uploads/directorate/stat_econ/IRSP_2016-17/Facts_Figure/Fact_Figures%20English%202016-17.pdf) accessed on 1st September 2020.
- [3] Pedrozo VB, May I, Macklini Dalla Nora AC, Zhao H. Experimental analysis of ethanol dual-fuel combustion in a heavy-duty diesel engine: an optimization at low load. *Appl Energy* 2016;165:166–82. <https://doi.org/10.1016/j.apenergy.2015.12.052>.
- [4] Interim Report- Exhaust Emission Benchmarks for Diesel Locomotives on Indian Railways. Available From: [http://www.indiaenvironmentportal.org.in/files/file/Draft\\_Interim\\_Rly\\_Diesel\\_Emission\\_Std.pdf](http://www.indiaenvironmentportal.org.in/files/file/Draft_Interim_Rly_Diesel_Emission_Std.pdf) accessed on 1st September 2020.
- [5] Indian Railway yearbook 2017-18. Available From: [http://www.indianrailways.gov.in/railwayboard/view\\_section.jsp?lang=0&id=0,1,304,366,554](http://www.indianrailways.gov.in/railwayboard/view_section.jsp?lang=0&id=0,1,304,366,554) accessed on 1st September 2020.
- [6] Valera H, Agarwal AK. Methanol as an alternative fuel for diesel engines. In: Agarwal A, Gautam A, Sharma N, Singh A, editors. *Methanol and the Alternate Fuel Economy, Energy, Environment, and Sustainability*. Singapore: Springer; 2019. p. 9–33. [https://doi.org/10.1007/978-981-15-0418-1\\_2](https://doi.org/10.1007/978-981-15-0418-1_2).
- [7] Valera H, Agarwal AK. Future automotive powertrains for india: methanol versus electric vehicles. In: Singh A, Sharma Y, Mustafi N, Agarwal A, editors. *Alternative Fuels and Their Utilization Strategies in Internal Combustion Engines*. Energy, Environment, and Sustainability. Singapore: Springer; 2020. p. 89–123. [https://doi.org/10.1007/978-981-15-0418-1\\_7](https://doi.org/10.1007/978-981-15-0418-1_7).
- [8] Important properties of different fuels Available From: <https://www.mandieslrb.com/docs/defaultsource/shopwaredocuments/using-methanol-fuel-in-the-man-b-w-me-lgi-series.pdf?sfvrsn=4>. accessed on 1st September 2020.
- [9] Valera H, Singh AP, Agarwal AK. Prospects of methanol-fuelled carburetted two wheelers in developing countries. In: Singh A, Sharma N, Agarwal R, Agarwal A, editors. *Advanced Combustion Techniques and Engine Technologies for the Automotive Sector, Energy, Environment, and Sustainability*. Singapore: Springer; 2020. p. 53–73. [https://doi.org/10.1007/978-981-15-0368-9\\_4](https://doi.org/10.1007/978-981-15-0368-9_4).
- [10] Qu X, Gong C, Liu J, Cui F, Liu F. Regulated and unregulated emissions from a DISI methanol engine under homogenous combustion and light load. *Fuel* 2015;158: 166–75. <https://doi.org/10.1016/j.fuel.2015.05.033>.
- [11] Gong CM, Li J, Li JK, Li WX, Gao Q, Liu XJ. Effects of ambient temperature on firing behavior and unregulated emissions of spark-ignition methanol and liquefied petroleum gas/methanol engines during cold start. *Fuel* 2011;90(1):19–25. <https://doi.org/10.1016/j.fuel.2010.08.012>.
- [12] Agarwal AK, Shukla PC, Gupta JG, Patel C, Prasad RK, Sharma N. Unregulated emissions from a gasohol (E5, E15, M5, and M15) fuelled spark ignition engine. *Appl Energy* 2015;154:732–41. <https://doi.org/10.1016/j.apenergy.2015.05.052>.
- [13] Gong C, Li Z, Yi L, Liu F. Experimental investigation of equivalence ratio effects on combustion and emissions characteristics of an H2/methanol dual-injection engine under different spark timings. *Fuel* 2020;262. <https://doi.org/10.1016/j.fuel.2019.116463>.
- [14] Gong C, Yi L, Zhang Z, Sun J, Liu F. Assessment of ultra-lean burn characteristics for a stratified-charge direct-injection spark-ignition methanol engine under different high compression ratios. *Appl Energy* 2020;261. <https://doi.org/10.1016/j.apenergy.2019.114478>.
- [15] Gong C, Zhang Z, Sun J, Chen Y, Liu F. Computational study of nozzle spray-line distribution effects on stratified mixture formation, combustion and emissions of a high compression ratio DISI methanol engine under lean-burn condition. *Energy* 2020;205. <https://doi.org/10.1016/j.energy.2020.118080>.
- [16] Gong C, Li Z, Sun J, Liu F. Evaluation on combustion and lean-burn limit of a medium compression ratio hydrogen/methanol dual-injection spark-ignition engine under methanol late-injection. *Appl Energy* 2020;277. <https://doi.org/10.1016/j.apenergy.2020.115622>.
- [17] Gong C, Sun J, Liu F. Numerical study of twin-spark plug arrangement effects on flame, combustion and emissions of a medium compression ratio direct-injection methanol engine. *Fuel* 2020;279. <https://doi.org/10.1016/j.fuel.2020.118427>.
- [18] Valera H, Kumar D, Agarwal AK. Feasibility Assessment of Methanol Fueling in Two-Wheeler Engine using 1-D Simulations. In Press. SAE Technical Paper 2021-01-0382. ISSN: 0148-7191, e-ISSN: 2688-3627.
- [19] Agarwal T, Singh AP, Agarwal AK. Development of port fuel injected methanol (M85)-fuelled two-wheeler for sustainable transport. *J. Traffic Transport. Eng (English Edition)* 2020;7(3):298–311. <https://doi.org/10.1016/j.jtte.2020.04.003>.
- [20] Agarwal AK, Karare H, Dhar A. Combustion, performance, emissions and particulate characterization of a methanol–gasoline blend (gasohol) fuelled medium duty spark ignition transportation engine. *Fuel Process Technol* 2014;121: 16–24. <https://doi.org/10.1016/j.fuproc.2013.12.014>.
- [21] Kumar D, Valera H, Agarwal AK. Numerical Predictions of In-cylinder Phenomenon in Methanol Fueled Locomotive Engine using High Pressure Direct Injection Technique. In Press. SAE Technical Paper 2021-01-0492. ISSN: 0148-7191, e-ISSN: 2688-3627.
- [22] Methanol as a potential alternative fuel for shipping: A brief talk with Chris Chatterton of the Methanol Institute. <https://www.dnvgl.com/maritime/advisor/y/af-update/Methanol-as-a-potential-alternative-fuel-for-shipping-A-brief-talk-with-Chris-Chatterton.html>. Accessed on 22nd January 2021.
- [23] Mitsubishi-Led Consortium Starts Up \$1-Billion Methanol-DME Plant In Trinidad And Tobago. [https://www.chemengonline.com/mitsubishi-led-consortium-starts-up-1-billion-methanol-dme-plant-in-trinidad-and-tobago/?oly\\_enc\\_id=1249J2867912G9F](https://www.chemengonline.com/mitsubishi-led-consortium-starts-up-1-billion-methanol-dme-plant-in-trinidad-and-tobago/?oly_enc_id=1249J2867912G9F). Accessed on 22nd January 2021.
- [24] Chao M, Lin T, Chao H, Chang F, Chen C. Effects of methanol containing additive on emission characteristics from a heavy-duty diesel engine. *Sci Total Environ* 2001; 279(1–3):167–79. [https://doi.org/10.1016/S0048-9697\(01\)00764-1](https://doi.org/10.1016/S0048-9697(01)00764-1).
- [25] Kumar MS, Ramesh A, Nagalingam B. An experimental comparison of methods to use methanol and jatropha oil in a compression ignition engine. *Biomass Bioenergy* 2003;25(3):309–18. [https://doi.org/10.1016/S0961-9534\(03\)00018-7](https://doi.org/10.1016/S0961-9534(03)00018-7).
- [26] Canakci M, Sayin C, Ozsezen AN, Turkcan A. Effect of injection pressure on the combustion, performance, and emission characteristics of a diesel engine fueled with methanol-blended diesel fuel. *Energy Fuels* 2009;23(6):2908–20. <https://doi.org/10.1021/ef900060s>.
- [27] Ciniviz M, Kose H, Canli E, Solmaz O. An experimental investigation on effects of methanol blended diesel fuels to engine performance and emissions of a diesel engine. *Sci Res Essays* 2011;6(15):3189–99. <https://doi.org/10.5897/SRE11.230>.
- [28] Agarwal AK, Shukla PC, Patel C, Gupta JG, Sharma N, Prasad RK, Agarwal RA. Unregulated emissions and health risk potential from biodiesel (KBS, KB20) and methanol blend (M5) fuelled transportation diesel engines. *Renew Energy* 2016;98: 283–91. <https://doi.org/10.1016/j.renene.2016.03.058>.
- [29] Qi DH, Chen H, Geng LM, Bian YZH, Ren XC. Performance and combustion characteristics of biodiesel-diesel-methanol blend fuelled engine. *Appl Energy* 2010;87(5):1679–86. <https://doi.org/10.1016/j.apenergy.2009.10.016>.
- [30] Zhu L, Cheung CS, Zhang WG, Huang Z. Emission's characteristics of a diesel engine operating on biodiesel and biodiesel blended with ethanol and methanol. *Sci Total Environ* 2010;408(4):914–21. <https://doi.org/10.1016/j.scitotenv.2009.10.078>.
- [31] Yasin MH, Yusaf T, Mamat R, Fitri YA. Characterization of a diesel engine operating with a small proportion of methanol as a fuel additive in biodiesel blend. *Appl Energy* 2014;114:865–73. <https://doi.org/10.1016/j.apenergy.2013.06.012>.
- [32] Bharadwaz YB, Rao BG, Rao VD, Anusha C. Improvement of biodiesel methanol blends performance in a variable compression ratio engine using response surface methodology. *Alexand Eng J* 2016;55(2):1201–9. <https://doi.org/10.1016/j.aej.2016.04.006>.

[33] Prashant GK, Lata DB, Joshi PC. Investigations on the effect of methanol blend on the combustion parameters of dual fuel diesel engine. *Appl Therm Eng* 2016;103:187–94. <https://doi.org/10.1016/j.applthermaleng.2016.04.061>.

[34] Huang ZH, Lu HB, Jiang DM, Zeng K, Liu B, Zhang JQ, Wang XB. Engine performance and emissions of a compression ignition engine operating on the diesel–methanol blends. *Proc Inst Mech Eng Part D J Automobile Eng* 2004;218(4):435–47. <https://doi.org/10.1243/09544070477359944>.

[35] Agarwal AK, Sharma N, Singh AP, Kumar V, Satsangi DP, Patel C. Adaptation of methanol–dodecanol–diesel blend in diesel genset engine. *J Energy Res Technol* 2019;141(10). <https://doi.org/10.1115/1.4043390>.

[36] Valera, H. An experimental study on the physico-chemical properties, performance parameter in a CI engine fuelled with methanol blended diesel (MBD) M.Tech Thesis, Department of Mechanical Engineering, Dr. B.R. Ambedkar National Institute of Technology (India), August 2017.

[37] Ning L, Duan Q, Chen Z, Kou H, Liu B, Yang B, Zeng K. A comparative study on the combustion and emissions of a non-road common rail diesel engine fueled with primary alcohol fuels (methanol, ethanol, and n-butanol)/diesel dual fuel. *Fuel* 2020;266. <https://doi.org/10.1016/j.fuel.2020.117034>.

[38] Li G, Zhang C, Li Y. Effects of diesel injection parameters on the rapid combustion and emissions of an HD common-rail diesel engine fueled with diesel-methanol dual-fuel. *Appl Therm Eng* 2016;108:1214–25. <https://doi.org/10.1016/j.applthermaleng.2016.08.029>.

[39] Yao C, Cheung CS, Cheng C, Wang Y, Chan TL, Lee SC. Effect of diesel/methanol compound combustion on diesel engine combustion and emissions. *Energy Convers Manage* 2008;49(6):1696–704. <https://doi.org/10.1016/j.enconman.2007.11.007>.

[40] Song R, Liu J, Wang L, Liu S. Performance and emissions of a diesel engine fuelled with methanol. *Energy Fuels* 2008;22(6):3883–8. <https://doi.org/10.1021/ef800492r>.

[41] Cheng CH, Cheung CS, Chan TL, Lee SC, Yao CD. Experimental investigation on the performance, gaseous and particulate emissions of a methanol fumigated diesel engine. *Sci Total Environ* 2008;389(1):115–24. <https://doi.org/10.1016/j.scitotenv.2007.08.041>.

[42] Yao C, Cheung CS, Cheng C, Wang Y. Reduction of smoke and NOx from diesel engines using a diesel/methanol compound combustion system. *Energy Fuels* 2007;21(2):686–91. <https://doi.org/10.1021/ef0602731>.

[43] Pan W, Yao C, Han G, Wei H, Wang Q. The impact of intake air temperature on performance and exhaust emissions of a diesel methanol dual fuel engine. *Fuel* 2015;162:101–10. <https://doi.org/10.1016/j.fuel.2015.08.073>.

[44] Shamon S, Hasimoglu C, Murcak A, Andersson O, Tuner M. Experimental investigation of methanol compression ignition in a high compression ratio HD engine using a Box-Behnken design. *Fuel* 2017;209:624–33. <https://doi.org/10.1016/j.fuel.2017.08.039>.

[45] Geng P, Yao C, Wei L, Liu J, Wang Q, Pan W, Wang J. Reduction of PM emissions from a heavy-duty diesel engine with diesel/methanol dual fuel. *Fuel* 2014;123:1–11. <https://doi.org/10.1016/j.fuel.2014.01.056>.

[46] Wang Y, Wang H, Meng X, Tian J, Wang Y, Long W, Li S. Combustion characteristics of high pressure direct-injected methanol ignited by diesel in a constant volume combustion chamber. *Fuel* 2019;254. <https://doi.org/10.1016/j.fuel.2019.06.006>.

[47] Jia Z, Denbratt I. Experimental investigation into the combustion characteristics of a methanol-Diesel heavy duty engine operated in RCCI mode. *Fuel* 2018;226:745–53. <https://doi.org/10.1016/j.fuel.2018.03.088>.

[48] Dong Y, Kaario O, Hassan G, Ranta O, Larmi M, Johansson B. High-pressure direct injection of methanol and pilot diesel: A non-premixed dual-fuel engine concept. *Fuel* 2020;277. <https://doi.org/10.1016/j.fuel.2020.117932>.

[49] Effects of Injection Timing of Diesel Fuel On Performance And Emission Of Dual Fuel Diesel Engine Powered By Diesel/E85. *Fuels Transport* 2018;33(3):633–646. <https://doi.org/10.3846/transport.2018.1572>.

[50] Wartsila Gas Engine Development and Methanol Adaptation, Classnk Seminar, Singapore 3.11.2015. Available From: [https://www.classnk.or.jp/classnk-rd/assets/pdf/V\\_Wartsila\\_Gas\\_Engine\\_Development\\_Methanol\\_Adaptation.pdf](https://www.classnk.or.jp/classnk-rd/assets/pdf/V_Wartsila_Gas_Engine_Development_Methanol_Adaptation.pdf) accessed on 1st September 2020.

[51] Rahman KA, Ramesh A. Studies on the effects of methane fraction and injection strategies in a biogas diesel common rail dual fuel engine. *Fuel* 2019;236:147–65. <https://doi.org/10.1016/j.fuel.2018.08.091>.

[52] Liu J, Yang F, Wang H, Ouyang M, Hao S. Effects of pilot fuel quantity on the emissions characteristics of a CNG/ diesel dual fuel engine with optimized pilot injection timing. *Appl Energy* 2013;110:201–6. <https://doi.org/10.1016/j.apenergy.2013.03.024>.

[53] Schlatter S, Schneider B, Wright YM, Boulouchos K. N-heptane micro pilot assisted methane combustion in a rapid compression expansion machine. *Fuel* 2016;179:339–52. <https://doi.org/10.1016/j.fuel.2016.03.006>.

[54] Dong S, Wang Z, Yang C, Ou B, Lu H, Xu H, Cheng X. Investigations on the effects of fuel stratification on auto-ignition and combustion process of an ethanol/diesel dualfuel engine. *Appl Energy* 2018;230:19–30. <https://doi.org/10.1016/j.apenergy.2018.08.082>.

[55] Boretti A. Advantages of converting diesel engines to run as dual fuel ethanol-diesel. *Appl Therm Eng* 2012;47:1–9. <https://doi.org/10.1016/j.applthermaleng.2012.04.037>.

[56] Sarjovaara T, Alantie J, Larmi M. Ethanol dual-fuel combustion concept on heavy duty engine. *Energy* 2013;63:76–85. <https://doi.org/10.1016/j.energy.2013.10.053>.

[57] Sahoo B, Sahoo N, Saha U. Effect of engine parameters and type of gaseous fuel on the performance of dual-fuel gas diesel engines—a critical review. *Renew Sustain Energy Rev* 2009;13(6–7):1151–84. <https://doi.org/10.1016/j.rser.2008.08.003>.

[58] Valera H, Kumar D, Singh A.P., Agarwal A.K. Modelling Aspects for Adaptation of Alternative Fuels in IC Engines. In: Singh A., Shukla P., Hwang J., Agarwal A. (eds) Simulations and Optical Diagnostics for Internal Combustion Engines. Energy, Environment, and Sustainability. Springer, Singapore 2020;9–26. [https://doi.org/10.1007/978-981-15-0335-1\\_2](https://doi.org/10.1007/978-981-15-0335-1_2).

[59] Heywood, J.B., 1988. Combustion engine fundamentals.

[60] GT-Power Software- Engine Performance Application Manual Version 2018. From <https://www.gtisoft.com/> accessed on 1st September 2020.

[61] Ajav EA, Singh B, Bhattacharya TK. Performance of a stationary diesel engine using vaporized ethanol as supplementary fuel. *Biomass Bioenergy* 1998;15(6):493–502. [https://doi.org/10.1016/S0961-9534\(98\)00055-5](https://doi.org/10.1016/S0961-9534(98)00055-5).

[62] Andrea TD, Henshaw PF, Ting DS. The addition of hydrogen to gasoline-fuelled SI engine. *Int J Hydrogen Energy* 2004;29(14):1541–52. <https://doi.org/10.1016/j.ijhydene.2004.02.002>.